J Biochem Tech (2019) 10(3): 56-65
ISSN: 0974-2328

Computational Study of Interaction between Olfactory Chemokine Receptor and Dienone Musks

Kamel Benmiloud*, Meriam Merad, Said Ghalem

Received: 16 May 2019 / Received in revised form: 12 September 2019, Accepted: 15 September 2019, Published online: 26 September 2019

Abstract

Smell is an important human sense for a comfortable life which interested perfume and luxury industries till now. In this paper, we investigated theoretically interactions between chemokine receptor and synthetic odorants of the young family of dienone musks using molecular docking by exploring the steric and electrostatic complementarity. Interpreted results allowed better understanding of smelling process involving protein receptors and brought helpful ideas to design new odorant molecules.

Keywords: Smell- chemokine-olfaction- musks- molecular docking

Introduction

The odor molecules are interpreted by man. The main organ involved in this processes is brain which previously has recorded odors and stored in memorial system, allowing human to express many emotions (Charlier, 2009). However, the odorant molecules of different families share different characteristics in structure and solubility (Dravnieks, 1974). The perception of smell is the result of at least three steps, involved sequentially after an odorant has reached the olfactory region (Charlier, 2009). The first one is detection and the two other steps, namely transduction and signal integration, both involve neuronal or even higher level protagonists, but do not involve odorants (Golebiowski et al., 2012). Detection is the most important step for chemists working in the field of flavor and fragrance, since it represents the primary link between the odorant and the full perception process. Odorant detection is usually thought to solely correspond to the chemoreception of odorants by olfactory receptors, which are indeed the main protagonists of the molecular step in the perception of smell (Buck and Axel, 1991; Meierhenrich et al., 2004).

The olfactory apparatus in vertebrates is capable of distinguishing and recognizing thousands of volatile chemicals at different structures and this chemosensory function is characterized by a very large family of odor receptors with seven transmembranes encoded by about 1000 genes, the majority of which would be pseudogenes in humans (Zozulya, Echeverri and Nguyen, 2001; Zhang and Firestein, 2002; Niimura et al., 2003; Godfrey, Malnic and Buck, 2004; Malnic, Godfrey and Buck, 2004; Olender *et al.*, 2004), spurred a burgeoning research effort in domains ranging from the neurosciences to clinical applications.

However, the understanding of the mechanisms underlying the role of olfactory receptor genes prevents several problems. Among these concerns is how the discrimination of tens of thousands of odorants (combined into odors) is facilitated by a few hundred receptors (Crasto, Singer and Shepherd, 2001). Considering the recent discovery of nearly 5000 olfactory receptors (ORs) identified within the elephant genome, approximately 2000 of which are functional (Niimura, Matsui and Touhara, 2014). This is more than twice the number of functional ORs identified in mouse, rat or dog genomes. The human genome contains far fewer functional ORs (Zozulya, Echeverri and Nguyen, 2001; Niimura and Nei;2003 , Malnic, Godfrey and Buck, 2004; Glusman et al.2000 ,).

In recent years, significant efforts have been sought to provide a mechanistic basis for OR-odorant interactions at a molecular level through computational methods (Lai, Singer and Crasto, 2005; Lai and Crasto, 2012; Lai et al., 2014; Floriano et al., 2000; Vaidehi et al., 2002; Floriano, Vaidehi and Goddard, 2004). These methods have involved creating OR protein models and simulating interactions with odorants using static or dynamic methods. Modeling studies are essential as they provide a mechanistic view of OR-odorant interactions at the molecular level. Different methodologies have been adopted for creating OR models.

Kamel Benmiloud*

Laboratory of Natural and bio-actives Substances, Tlemcen University- Faculty of Science. P.O.Box 119-Tlemcen-Algeria.
Laboratory of Naturals Products and Bio actives-LASNABIO-Faculty of Science- Department of Chemistry-University Aboubekr Belkaid-Tlemcen- Algeria

Meriam Merad, Said Ghalem

Laboratory of Natural and bio-actives Substances, Tlemcen University- Faculty of Science. P.O.Box 119-Tlemcen-Algeria.

***Email:** kamel_benmiloud @ yahoo.fr

Although there is no direct evidence to support their functional role, OBPs appear as good candidates for the transport of odorants from the inhaled air to the bottom of the nasal mucus, where the olfactory neurons cilia expressing olfactory receptors are located **(**Golebiowski et al., 2012**)** (Figure 1).

The development and evolution of olfactory resources are more effective and more sustainable; and to understand the relationship, structure-smell represent important problems to solve and understand; there are several similar works to this idea such as the works of Jerome and his collaborators (March et al., 2015; Bushdid et al., 2019; Cong, Fiorucci and Golebiowski, 2018).

To the best of our knowledge our study is the first concerning chemokine interactions with dienone musks by computational methods.

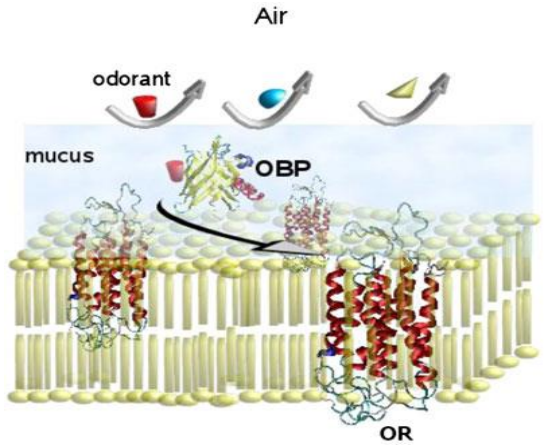

Figure 1: Odorant binding proteins (OBPs) in the nasal mucus capture odorants to putatively transport them to olfactory receptors (ORs) **(**Golebiowski et al., 2012**)**

Materials and Methods:

Molecular docking is important tool to understand interaction mechanisms in biological systems by computational methods. It is also used in many fields. Likewise, new molecules with biological activity have been discovered by studying complex formation and stability. Many docking programs (academic and commercial) are used to study interaction between protein receptor and molecules (MOE, 2014). In this paper we used Molecular Operating Environment software (MOE). Docking can be achieved via two important steps: first; sampling conformation of the ligand in the active site of the protein, then ranking these conformations via scoring function.

Description of the chemokine receptor (PDB CXCR4):

The chemokine receptor CXCR4 is a 352 amino acid rhodopsin-like GPCR (Busillo and Benovic, 2007) and selectively binds the CXC chemokine Stromal Cell-Derived Factor 1 (SDF-1) also known as CXCL12 (Murphy et al., 2000). All 397 human OR sequences were aligned with the sequence of GPCRs for which the experimental structure is known. Manual adjustments were performed to be consistent with the data from 141 mutants previously described in the literature. A homology model was obtained using the crystal structures CXCR4 chemokine receptor (3ODU) as structural templates using Modeler.

Preparation and optimization of both enzyme and ligands

Three dimensional structure of CXCR4 was downloaded from PROTEIN DATA BANK under code 3ODU with x-ray resolution equal to 2.5 Å. We note that the CXCR4 crystallizes as a monomer (Fig. 2) with residues and atoms (Desjardins et al., 2007; Wu et al., 2010; Wu et al., 2010). Ligands listed in table 2 were selected from literature (Kraft and Popaj, 2008) and drawn using build module implanted in MOE software, and their characteristics are shown in table 1.

Energy and geometry of the enzyme was performed using AMBER force filed and Hamiltonian AM1 implanted in MOE under default parameters (300K, pH = 7), then the active site was identified and isolated using site finder module as shown in figures 3.

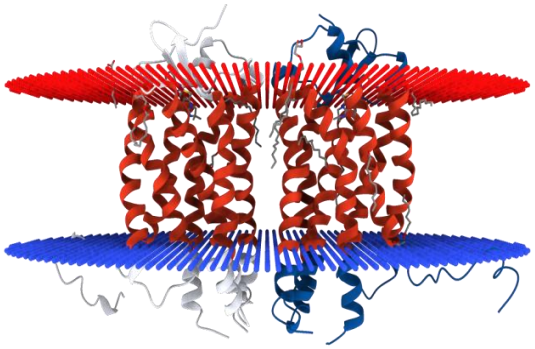

Figure 2: Simplified model of CXCR4 enzyme under PDB code 3ODU.

Docking

The docking consists into positioning of the ligands in the active site in order to establish a favorable conformational binding between ligands and the enzyme (Clark and Labute, 2009) using dock module implanted in MOE.

Table 1: Molecular descriptors analysis of 13 ligands using MOE software

Ligand	MW	LogP	LogS	TPSA	H-bonds donors	H-bands acceptors	Toxicity
1	294.30	3.62	-5.30	108.71	0	1	NO
2	258.40	5.41	-6.77	9.23	0	1	NO
3	240.38	4.61	-5.27	36.30	0	1	NO
4	256.34	3.09	-4.15	52.60	0	2	NO

5	284.43	4.34	-4.54	35.53	0	2	NO
6	268.39	4.34	-4.64	35.53	0	2	NO
7	268.39	3.73	-3.31	35.53	0	2	NO
8	270.36	3.09	-4.15	52.60	0	2	NO
9	250.37	3.77	-4.19	18.46	0	2	NO
10	196.33	3.76	-4.80	17.07	0	1	NO
11	208.34	4.15	-5.31	17.07	0	1	NO
12	220.36	4.29	-4.91	17.07	0	1	NO
13	206.33	3.90	-4.40	17.07	0	1	NO

MW: Molecular weight (g/mol), TPSA: Polar surface area (Å^2), logP: Octanol-water partition coefficient, logS: aqueous solubility, H- bonds donors: Number of H- bonds donors, H-bonds acceptors: Number of H- bonds acceptors.

Tableau 2: List of ligands

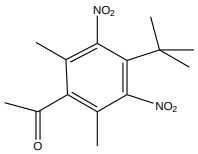	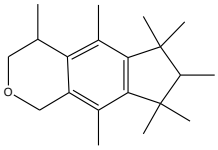	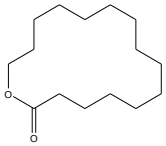
L1	L2	L3
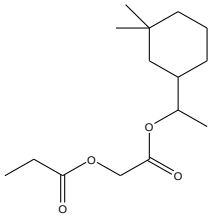	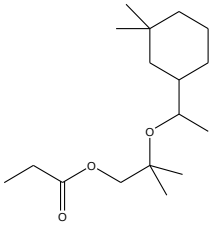	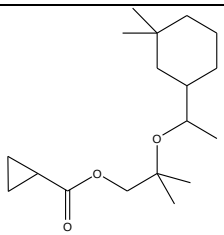
L4	L5	L6
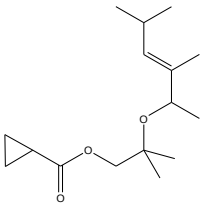	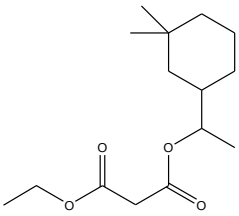	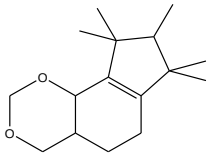
L7	L8	L9
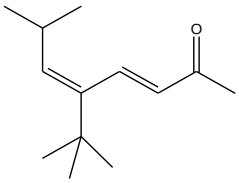	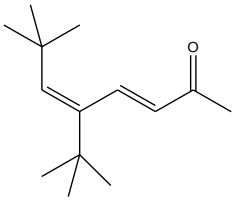	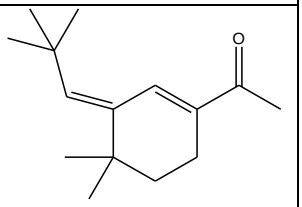
L10	L11	L12
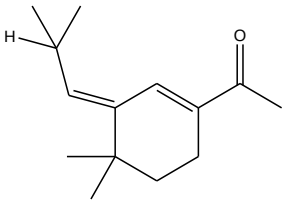		
L13		

Tableau 3: Physico-chemical properties of odorant ligands

Ligants	**IUPAC Name**	**Pubchem CID**	**Molar mass (g/mol)**	**formula**

L1	1-(4-tert-butyl-2,6-dimethyl-3,5-dinitrophenyl)ethanone	6669	294.30	$C_{14}H_{18}N_2O_5$
L2	4,6,6,7,8,8-hexamethyl-1,3,4,7-tetrahydrocyclopenta[g]isochromene	91497	258.40	$C_{18}H_{26}O$
L3	oxacyclohexadecan-2-one	235414	240.38	$C_{15}H_{28}O_2$
L4	1-(3,3-dimethylcyclohexyl)ethyl 2-acetyloxyacetate	132530715	256.34	$C_{14}H_{24}O_4$
L5	2-[1-(3,3-Dimethylcyclohexyl)ethoxy]-2-methylpropyl propionate	16063567	284.43	$C_{17}H_{32}O_3$
L6	[2-[(E)-3,5-dimethylhex-3-en-2-yl]oxy-2-methylpropyl] cyclopropanecarboxylate	11277198	268.39	$C_{16}H_{28}O_3$
L7	2-methyl-2-((1,2,4-trimethyl-2-penten-1-yl)oxy)propyl ester	11277198	268.39	$C_{16}H_{28}O_3$
L8	3-*O*-[1-(3,3-dimethylcyclohexyl)ethyl] 1-*O*-ethyl propanedioate	57759198	270.36	$C_{15}H_{26}O_4$
L9	7,7,8,9,9-pentamethyl-4,4a,5,6,8,9b-hexahydrocyclopenta[h][1,3]benzodioxine	15552386	250.37	$C_{16}H_{26}O_2$
L10	5-tert-butyl-7-methylocta-3,5-dien-2-ol	71424975	196.33	$C_{13}H_{24}O$
L11	5-tert-butyl-7,7-dimethylocta-3,5-dien-2-one	71424970	208.34	$C_{14}H_{24}O$
L12	(3'E)-1-[4',4'-Dimethylcyclohex-1'-enyl-3'-(2'',2''-dimethylpropylidene)] ethanone	/	220.36	$C_{15}H_{27}O$
L13	(3'E)-1-[4',4'-Dimethyl-3'-(2''-methylpropylidene)cyclohex-1'-enyl]-ethanone	/	206.33	$C_{14}H_{15}O$

Results and Discussion

The results obtained are ranked in descending order in Table 4. The structure of the molecules plays an important role in the positioning of the odorant ligands in the active site of the enzyme. It can be concluded that the introduction of bulky groups causes a rearrangement of conformation within the cavity of the active site, which will probably be the complementarity and therefore the activity. The two-dimensional molecular method of the screen has been attributed to the MOE software, designed to visualize the active sites of the complex (protein-ligand). The ligand is prepared and manufactured with an improved 2D representation layout algorithm, and a version of the protein residues is arranged around it to indicate the spatial proximity of the links (Clark and Labute, 2009). If there are multiple channels in the system, positions are preceded by letters of the alphabet. Interactions between 2.5 Å and 3.1 Å are considered high and those between 3.1Å and 3.55Å are average. The interactions greater than 3.55Å are weak (Ritchie and Kemp, 2000).

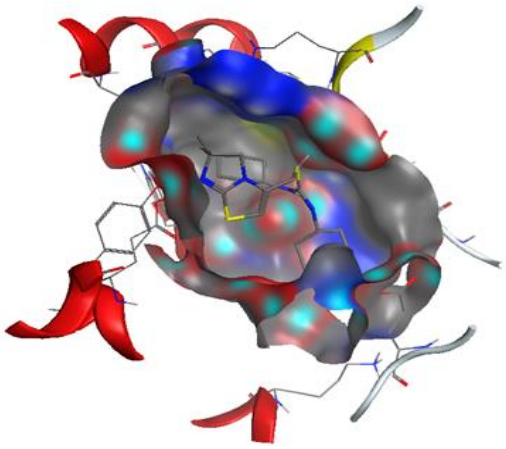

Figure 3: Isolated active site of CXCR4 enzyme.

The enzyme - L7 complex (Fig 4) interacts with amino acids, [GLU 288 (A) H-acceptor], [TRP 94 (A) Pi-H], at a distance of 3.16 Å, and 4.04 Å, respectively for the 1st mean interaction and 2nd weak interaction, suggesting that L7 ligand may be the best inhibitor of CXCR4 (Yamaguchi et al., 2014).

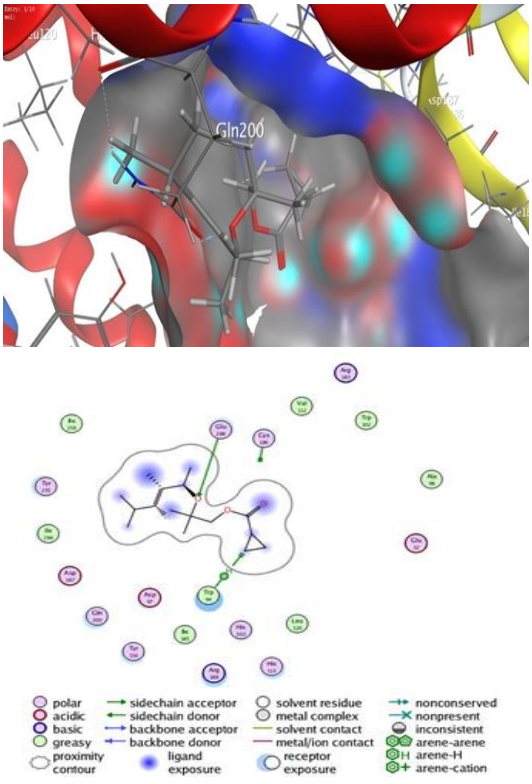

Figure 4: Diagram interaction of CXCR4 + L7.

For the enzyme-ligand complexes L12 and L11 (Fig 5, 6), we did not find any bonding for the two complexes formed; but the only possible forces are electric (Glu 288 and Cys 186), with total energies for the complexes -4.9191 Kcal/mol; -5.0816 Kcal/mol, respectively, which are low compared with the others (Table 4). For the other complexes formed, the bonds and types of bonds formed with amino acids are summarized and inserted in Table 4. The results revealed that the ligand L7 would be the best odor, which was confirmed by their weakest energies -6.5731 Kcal / mol.

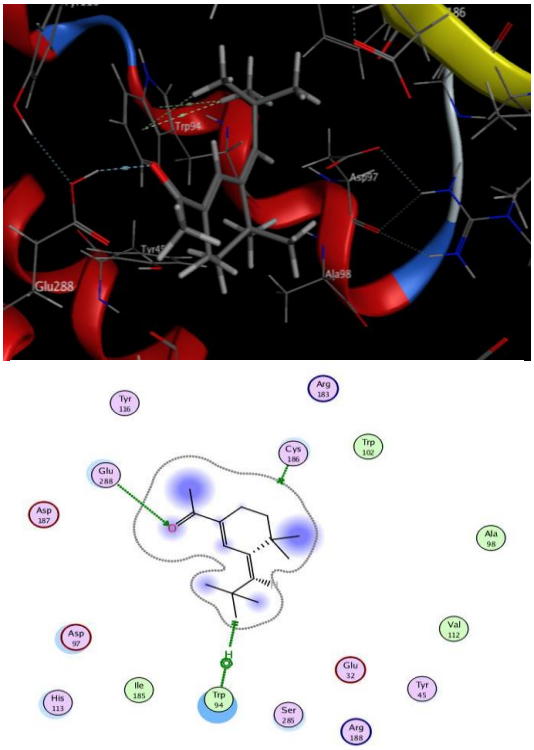

Figure 5: Diagram interaction of CXCR4+ L12.

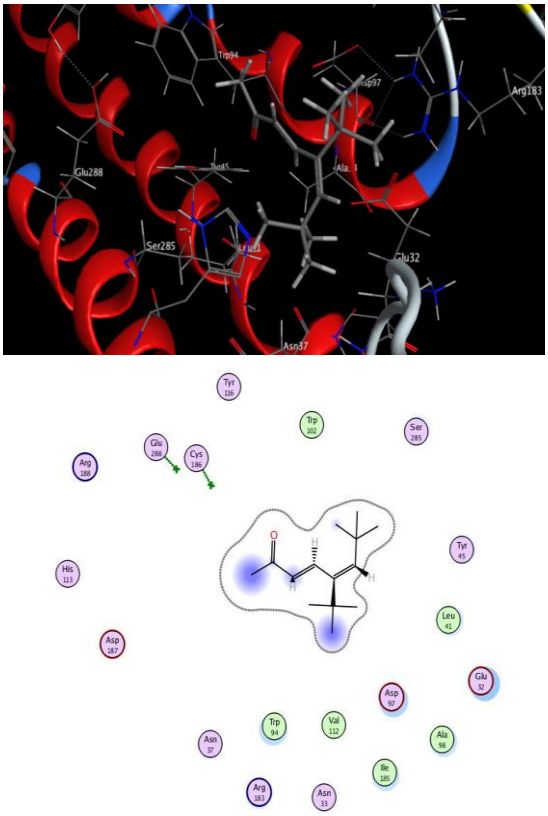

Figure 6: Diagram interaction of CXCR4+ L11.

Table 4: Results of score Enzyme – ligands

Compose	Score	RMSD	Distance	Energy of the distance (Kcal/mol)	Type of interaction	Amino acid bond	Type of bond
Ref - ligand	**-6.4566**	**6.0116**	**3.28** **3.81**	**-1.9** **-1.4**	**Mean** **Absent**	**Glu 288** **Cys 186**	**H-acceptor** **H-donor**
L9	-4.2717	2.9242	3.13 4.03	-1.2 -0.6	Mean Absent	Glu 288 Trp 94	H-acceptor Pi- H
L12	-4.7634	2.8529	3.01 4.09 4.11	-1.5 -0.8 -0.7	Strong Absent Absent	Glu 288 Trp 94 Trp 94	H-acceptor Pi- H Pi- H
L2	-4.7666	1.4525	4.06	-0.8	Absent	Glu 288	Pi- H
L10	-4.9191	2.0776	/	/	/	Glu 288 Cys 186	Force electric
L3	-4.9551	2.4397	4.07	-0.8	Absent	Trp 94	Pi- H
L13	-4.9996	1.1229	2.80 4.22	-4.9 -0.6	Strong Absent	Glu 288 Trp 94	Pi- H Pi- H
L11	-5.0816	1.0065	/	/	/	Glu 288	electric

						Cys 186	Force
L5	-5.4131	1.7104	3.86	-0.9	Absent	His 113	Pi- H
L8	-5.5317	1.6436	2.79	-2.6	Strong	Glu 288	H-acceptor
			4.03	-0.8	Absent	Trp 94	Pi- H
			4.00	-0.7	Absent	Trp 94	Pi- H
L1	-5.5758	1.2898	3.05	-1.6	Strong	Glu 288	H-acceptor
L6	-5.6162	1.6605	2.92	-1.2	Strong	Glu 288	H-acceptor
			3.99	-0.7	Absent	Trp 94	Pi- H
			3.99	-0.9	Absent	Trp 94	Pi- H
L4	-5.6403	2.1331	3.90	-0.8	Absent	His 113	Pi- H
			4.00	-0.7	Absent	Trp 94	Pi- H
L7	**-6.5731**	**2.0822**	**3.16**	**-1.3**	**Mean**	**Glu 288**	**H-acceptor**
			4.04	**-0.6**	**Absent**	**Trp 94**	**Pi- H**

For the CXCR4 + L9 complex (Fig 7): the ligand interacts with the amino acids [Glu 288 (H-acceptor), Trp 94 (Pi- H)] at distances of 3.13 Å, and 4.03Å respectively.

For the CXCR4 + L2 complex (Fig 8): the ligand interacts with the amino acid [Glu 288 (Pi- H)] at a distance of 4.06 Å.

For the CXCR4 + L10 complex (Fig 9): the ligand interacts with the amino acids [Glu 288 (H-acceptor), Trp 94 (Pi- H)] at a Force electric.

For the CXCR4 + L3 complex (Fig 11): the ligand interacts with the amino acid [Trp 94 (Pi- H)] at a distance of 4.07 Å.

For the CXCR4 + L13 complex (Fig 11): the ligand interacts with the amino acids [Glu 288 (Pi- H), Trp 94 (Pi- H)] at distances of 2.80 Å, and 4.22Å respectively.

For the CXCR4 + L5 complex (Fig 12): the ligand interacts with the amino acid [His 113 (Pi- H at a distance of 3.86 Å.

For the CXCR4 + L8 complex (Fig 13): the ligand interacts with the amino acids [Glu 288 (H-acceptor), Trp 94 (Pi- H), Trp 94 (Pi- H)] at distances of 2.79 Å, 4.03Å, and 4.00 Å respectively.

For the CXCR4 + L1 complex (Fig 14): the ligand interacts with the amino acid [Glu 288 (H-acceptor)] at a distance of 3.05 Å.

For the CXCR4 + L6 complex (Fig 15): the ligand interacts with the amino acids [Glu 288 (H-acceptor), Trp 94 (Pi- H), Trp 94 (Pi- H)] at distances of 2.92 Å, 3.99Å, and 3.99 Å respectively.

For the CXCR4 + L4 complex (Fig 16): the ligand interacts with the amino acids [His 113 (Pi- H), Trp 94 (Pi- H)] at distances of 3.90 Å, and 4.00Å respectively.

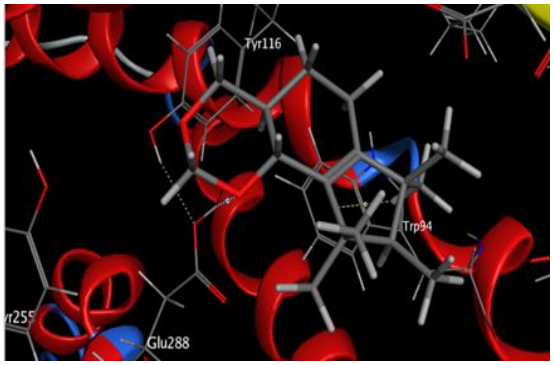

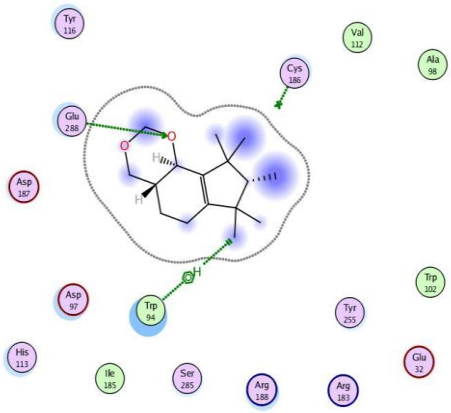

Figure 7: Diagram interaction of CXCR4 + L9.

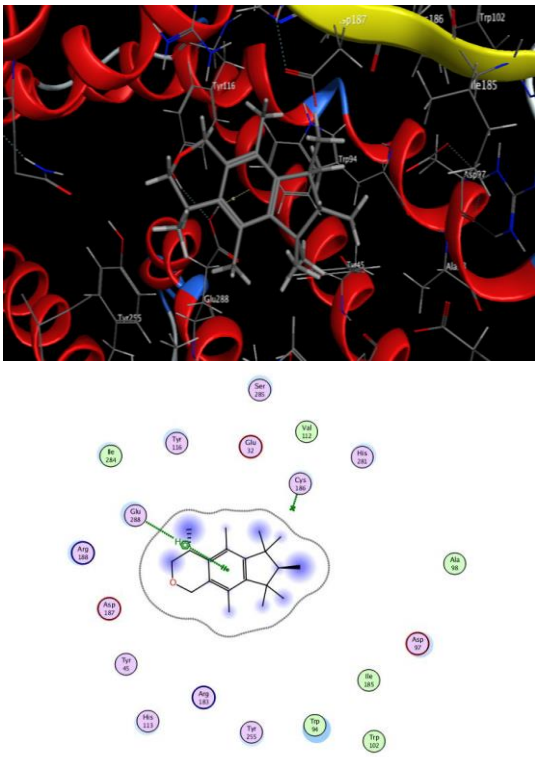

Figure 8: Diagram interaction of CXCR4 + L2

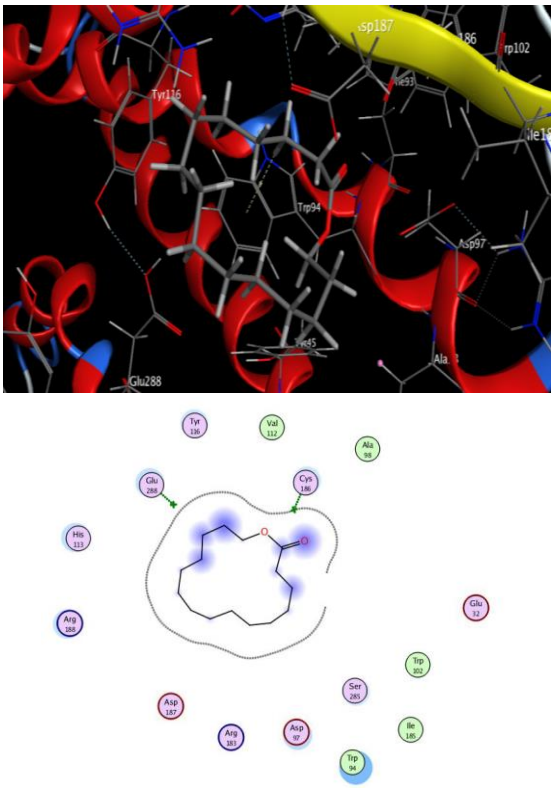

Figure 10: Diagram interaction of CXCR4 + L3

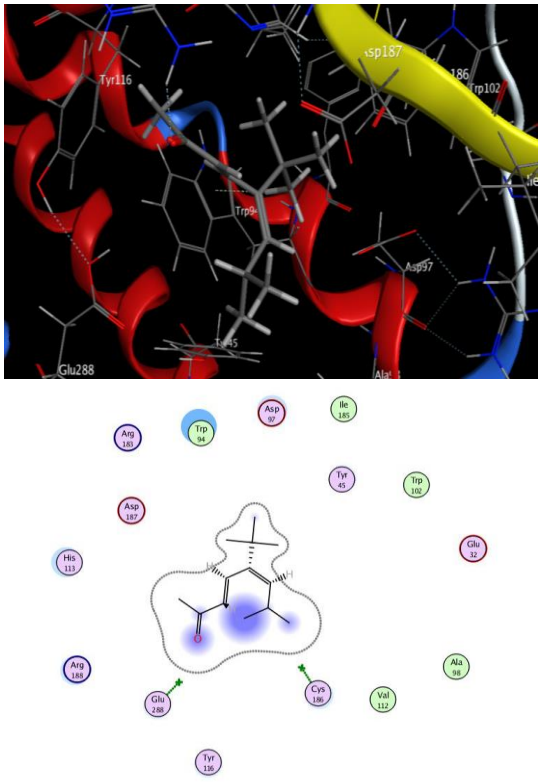

Figure 9: Diagram interaction of CXCR4+ L10.

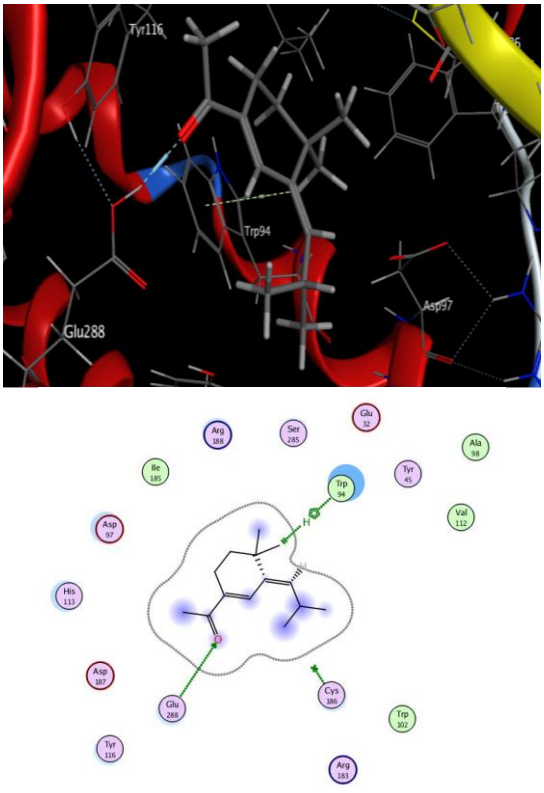

Figure 11: Diagram interaction of CXCR4+ L13.

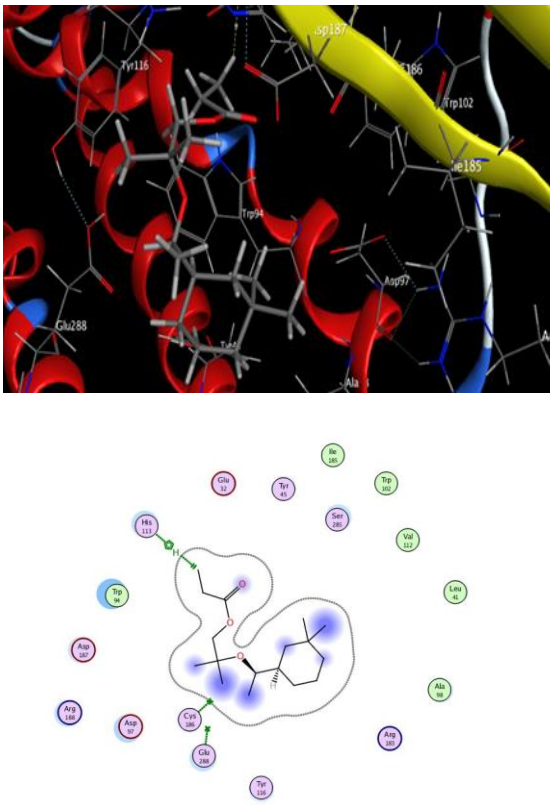

Figure 12: Diagram interaction of CXCR4 + L5

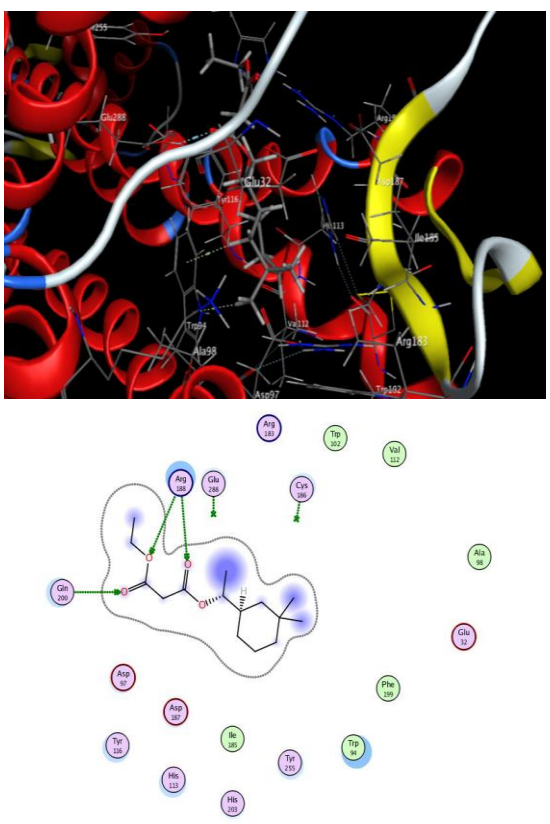

Figure 13: Diagram interaction of CXCR4 + L8

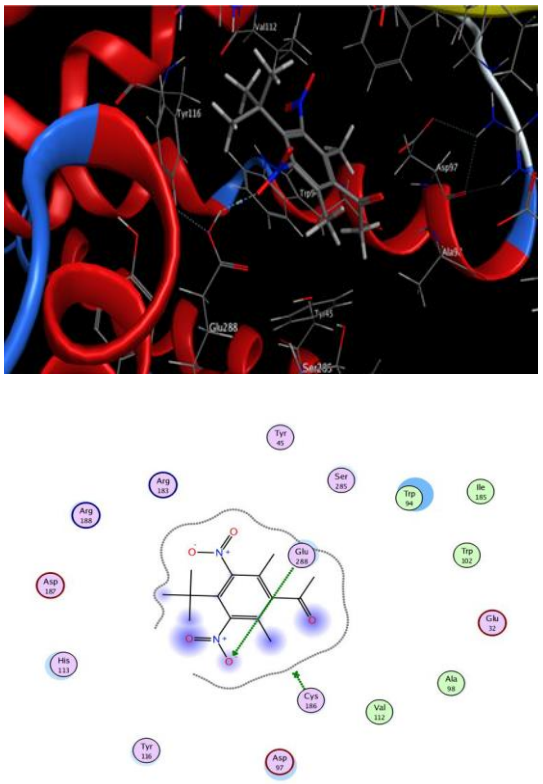

Figure 14: Diagram interaction of CXCR4 + L1

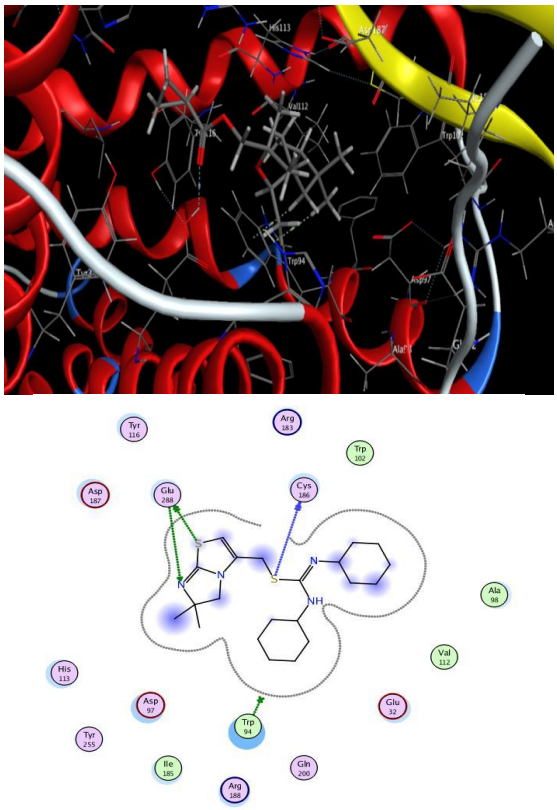

Figure 15: Diagram interaction of CXCR4 + L6

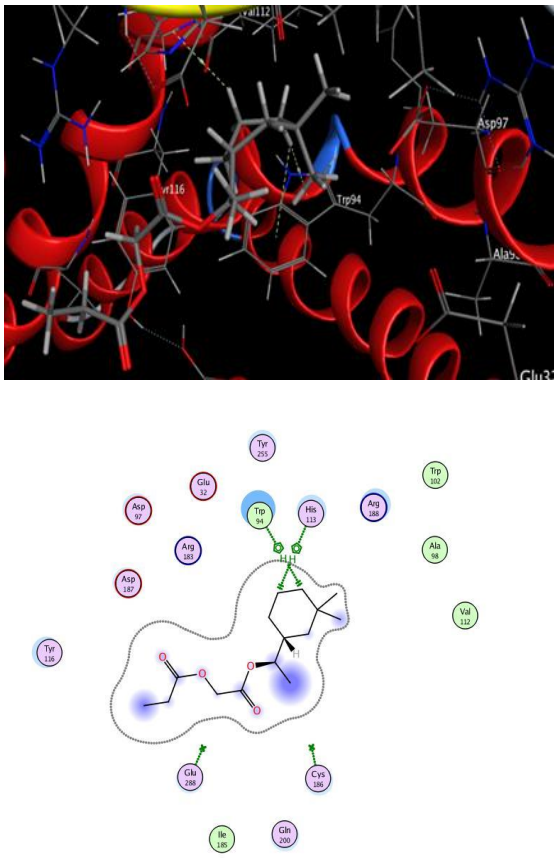

Figure 16: Diagram interaction of CXCR4 + L4.

Conclusion:

In this work, we studied the interaction of the olfactory enzyme by molecular docking. The results obtained allow us to conclude that the ligand L7 is the most stable one and may be the best inhibitor of CXCR4 in order to find the best odor.

Acknowledgement

Authors express their thanks to Doctor Salim Bouchentouf from Doctor Tahar Moulay University of saida and member of Laboratory of Natural products and bioacives for his valuable support.

References

Buck, L., & Axel, R. (1991). A novel multigene family may encode odorant receptors: a molecular basis for odor recognition. *Cell*, *65*(1), 175-187.

Bushdid, C., Claire, A., Topin, J., Do, M., Matsunami, H., & Golebiowski, J. (2019). Mammalian class I odorant receptors exhibit a conserved vestibular-binding pocket. *Cellular and molecular life sciences*, *76*(5), 995-1004.

Busillo, J. M., & Benovic, J. L. (2007). Regulation of CXCR4 signaling. *Biochimica et Biophysica Acta (BBA)-Biomembranes*, *1768*(4), 952-963.

Charlier, L. (2009). *Etude des Interactions moléculaires entre molécules odorantes et protéines impliquées dans les premières étapes de la perception olfactive* (Doctoral dissertation, Nice).

Clark, A. M., & Labute, P. (2008). Detection and assignment of common scaffolds in project databases of lead molecules. *Journal of medicinal chemistry*, *52*(2), 469-483.

Cong, X., Fiorucci, S., & Golebiowski, J. (2018). Activation dynamics of the neurotensin G protein-coupled receptor 1. *Journal of chemical theory and computation*, *14*(8), 4467-4473.

Crasto, C., Singer, M. S., & Shepherd, G. M. (2001). The olfactory receptor family album. *Genome biology*, *2*(10), reviews1027-1.

de March, C. A., Ryu, S., Sicard, G., Moon, C., & Golebiowski, J. (2015). Structure–odour relationships reviewed in the postgenomic era. *Flavour and Fragrance Journal*, *30*(5), 342-361.

Desjardins, S. F., Berchiche, Y. A., Haddad, E., & Heveker, N. (2007). CXCR4, un récepteur de chimiokine aux multiples talents. *médecine/sciences*, *23*(11), 980-984.

Dravnieks, A. (1974). A Building-Block Model for the Characterization of Odorant Molecules and Their Odors. *Annals of the New York Academy of Sciences*, *237*(1), 144-163.

Floriano, W. B., Vaidehi, N., & Goddard III, W. A. (2004). Making sense of olfaction through predictions of the 3-D structure and function of olfactory receptors. *Chemical senses*, *29*(4), 269-290.

Floriano, W. B., Vaidehi, N., Goddard, W. A., Singer, M. S., & Shepherd, G. M. (2000). Molecular mechanisms underlying differential odor responses of a mouse olfactory receptor. *Proceedings of the National Academy of Sciences*, *97*(20), 10712-10716.

Glusman, G., Sosinsky, A., Ben-Asher, E., Avidan, N., Sonkin, D., Bahar, A., ... & Demaille, J. (2000). Sequence, structure, and evolution of a complete human olfactory receptor gene cluster. *Genomics*, *63*(2), 227-245.

Godfrey, P. A., Malnic, B., & Buck, L. B. (2004). The mouse olfactory receptor gene family. *Proceedings of the National Academy of Sciences*, *101*(7), 2156-2161.

Golebiowski, J., Topin, J., Charlier, L., & Briand, L. (2012). Interaction between odorants and proteins involved in the perception of smell: the case of odorant-binding proteins probed by molecular modelling and biophysical data. *Flavour and Fragrance Journal*, *27*(6), 445-453.

Kraft, P., & Popaj, K. (2008). New Musk Odorants:(3E)-4-(2′-Alkyl-5′, 5′-dimethylcyclopent-1′-enyl) but-3-en-2-ones and (3E)-1-Acetyl-3-alkylidene-4, 4-dimethylcyclohexenes. *European Journal of Organic Chemistry*, *2008*(28), 4806-4814.

Lai, P. C., & Crasto, C. J. (2012). Beyond modeling: all-atom olfactory receptor model simulations. *Frontiers in genetics*, *3*, 61.

Lai, P. C., Guida, B., Shi, J., & Crasto, C. J. (2014). Preferential binding of an odor within olfactory receptors: a precursor to receptor activation. *Chemical senses*, *39*(2), 107-123.

Lai, P. C., Singer, M. S., & Crasto, C. J. (2005). Structural activation pathways from dynamic olfactory receptor–odorant interactions. *Chemical senses*, *30*(9), 781-792.

Malnic, B., Godfrey, P. A., & Buck, L. B. (2004). The human olfactory receptor gene family. *Proceedings of the National Academy of Sciences*, *101*(8), 2584-2589.

Meierhenrich, U. J., Golebiowski, J., Fernandez, X., & Cabrol-Bass, D. (2004). The molecular basis of olfactory chemoreception. *Angewandte Chemie International Edition*, *43*(47), 6410-6412.

Montreal (2014). Molecular operating environment (MOE) version 2014.09; Chemical Computing Group Inc.

Murphy, P. M., Baggiolini, M., Charo, I. F., Hébert, C. A., Horuk, R., Matsushima, K., ... & Power, C. A. (2000). International union of pharmacology. XXII. Nomenclature for chemokine receptors. *Pharmacological reviews*, *52*(1), 145-176.

Niimura, Y., & Nei, M. (2003). Evolution of olfactory receptor genes in the human genome. *Proceedings of the National Academy of Sciences*, *100*(21), 12235-12240.

Niimura, Y., Matsui, A., & Touhara, K. (2014). Extreme expansion of the olfactory receptor gene repertoire in African elephants and evolutionary dynamics of orthologous gene groups in 13 placental mammals. *Genome research*, *24*(9), 1485-1496.

Olender, T., Fuchs, T., Linhart, C., Shamir, R., Adams, M., Kalush, F., ... & Lancet, D. (2004). The canine olfactory subgenome. *Genomics*, *83*(3), 361-372.

Ritchie, D. W., & Kemp, G. J. (2000). Protein docking using spherical polar Fourier correlations. *Proteins: Structure, Function, and Bioinformatics*, *39*(2), 178-194.

Vaidehi, N., Floriano, W. B., Trabanino, R., Hall, S. E., Freddolino, P., Choi, E. J., ... & Goddard, W. A. (2002). Prediction of structure and function of G protein-coupled receptors. *Proceedings of the National Academy of Sciences*, *99*(20), 12622-12627.

Wu, B., Chien, E. Y., Mol, C. D., Fenalti, G., Liu, W., Katritch, V., ... & Hamel, D. J. (2010). Structures of the CXCR4 chemokine GPCR with small-molecule and cyclic peptide antagonists. *Science*, *330*(6007), 1066-1071.

Wu, B., Chien, E. Y., Mol, C. D., Fenalti, G., Liu, W., Katritch, V., ... & Hamel, D. J. (2010). Structures of the CXCR4 chemokine GPCR with small-molecule and cyclic peptide antagonists. *Science*, *330*(6007), 1066-1071.

Yamaguchi, H., Kamiie, K., Kidachi, Y., Noshita, T., Umetsu, H., Fuke, Y., & Ryoyama, K. (2014). Structural insight into the ligand-receptor interaction between 6-(methylsulfinyl) hexyl isothiocyanate and multidrug resistanceassociated protein 1 nucleotide-binding domain 1. *Int J Comput Bioinform In Silico Modeling*, *3*, 310-4.

Zhang, X., & Firestein, S. (2002). The olfactory receptor gene superfamily of the mouse. *Nature neuroscience*, *5*(2), 124.

Zozulya, S., Echeverri, F., & Nguyen, T. (2001). The human olfactory receptor repertoire. *Genome biology*, *2*(6), research0018-1.